Roles of Nucleoli in Germline Development of *Drosophila melanogaster*

A Dissertation Submitted to

the Graduate School of Life and Environmental Sciences,

the University of Tsukuba

in Partial Fulfillment of the Requirements

for the Degree of Doctor of Philosophy in Science

Shumpei MORITA

Abstract

In *Drosophila* ovary, germline stem cells (GSCs) divide to produce two daughter cells. One daughter is maintained as a GSC, whereas the other initiates cyst formation, a process involving four synchronous mitotic divisions that form 2-, 4-, 8-, and 16-cell cysts. In this study, I found that reduction in the level of *NHP2,* a component of the H/ACA small nucleolar ribonucleoprotein complex that catalyzes rRNA pseudouridylation, promotes progression to 8-cell cysts. NHP2 protein was concentrated in the nucleoli of germline cells during cyst formation. NHP2 expression, as well as the nucleolar size, abruptly decreased during progression from 2-cell to 4-cell cysts. Reduction in *NHP2* activity in the germline caused accumulation of 4- and 8-cell cysts and decreased the number of single cells. In addition, *NHP2* knockdown impaired the transition to 16-cell cysts. Furthermore, a tumorous phenotype caused by *Sex-lethal* (*Sxl*) knockdown, which is characterized by accumulation of single and 2-cell cysts, was partially rescued by *NHP2* knockdown. When *Sxl* and *NHP2* activities were concomitantly repressed, the numbers of 4- and 8-cell cysts were increased. In addition, Sxl protein physically interacted with *NHP2* mRNA in ovaries. Thus, it is reasonable to conclude that *Sxl* represses *NHP2* activity at the post-transcriptional level to promote proper cyst formation. Because *NHP2* knockdown did not affect global protein synthesis in the germarium, I speculate that changes in NHP2-dependent pseudouridylation, which is involved in translation of specific mRNAs, must be intact in order to promote proper cyst formation.

Introduction

In *Drosophila*, the adult ovary consists of approximately 20 elongated tubes, called ovarioles. At the distal tip of each ovariole is a germarium containing two or three germline stem cells (GSCs) (Fig. II-1A) (Lin, 1997; Xie and Spradling, 1998). GSCs asymmetrically divide to produce two daughter cells (Lin, 1997). The daughter cell adjacent to niche cells called cap cells is maintained as a GSC, whereas the other daughter cell (cystoblast) is detached from the niche, initiates differentiation, and undergoes cyst formation, a process involving four synchronous mitotic divisions with incomplete cytokinesis, to form 2-, 4-, 8-, and 16-cell cysts interconnected by fusomes (Lin et al., 1994; Robinson et al., 1994; de Cuevas et al., 1997) (Fig. II-1A). Among the 16 cells in a cyst, one differentiates into oocyte, and the other 15 become nurse cells that support oocyte maturation (Fig. II-1A).

A great deal of effort has been devoted to elucidating the mechanisms regulating GSC maintenance and self-renewal by short-range signals from the niche. GSC daughter cells that escape from the niche signal undergo differentiation and cyst formation (Fig. II-1A) (Kirilly and Xie 2007; Spradling *et al*. 2011). Upon differentiation, the daughter cell expresses *bag of marbles* (*bam*) gene, which is both necessary and sufficient for its differentiation (McKearin and Ohlstein 1995; McKearin and Spradling 1990; Ohlstein and McKearin 1997). This is supported by the fact that germline cells lacking *bam* function fail to progress through cyst formation, resulting in

over-proliferation of GSC-like single cells (McKearin and Ohlstein, 1995; McKearin and Spradling, 1990). By contrast, ectopic expression of *bam* in GSCs prevents these cells from maintaining stem cell identity (Ohlstein and McKearin, 1997). Transcriptional silencing of *bam* in GSCs is induced by the niche signal mediated by Decapentaplegic (Dpp), a member of the bone morphogenetic protein (BMP) ligand family (Chen and McKearin, 2003a). Once GSCs receive Dpp ligand from the niche, Mothers against dpp (Mad) protein is phosphorylated in GSCs, which in turn represses *bam* transcription by binding to a *bam* silencer element (Song et al., 2004).

However, the mechanism that regulates cyst formation and differentiation of GSC daughters remains to be fully elucidated. Recent studies have highlighted the roles of ribosome biogenesis and protein synthesis in control of the transition between GSC maintenance and differentiation (Xi et al., 2005; Zhang et al., 2014; Sanchez et al., 2016). For example, *under-developed* (*udd*) encodes a component of the RNA polymerase I regulatory complex, which is involved in rRNA transcription in nucleolus. Disruption of *udd* results in a reduction in Mad protein expression, which in turn prevents maintenance of GSCs (Zhang et al., 2014). This is compatible with the observation that GSCs retain a large nucleolus, and its size changes dynamically during cyst formation (Zhang et al., 2014; Sanchez et al., 2016). These data lead me to speculate that ribosome biogenesis occurring in the nucleolus may affect cyst formation and differentiation, in addition to GSC maintenance.

To address this issue, I focused on *NHP2*, a *Drosophila* homolog of yeast *Nhp2*, which is widely conserved among eukaryotes (FlyBase: www.flybase.org). The yeast Nhp2 protein is a component of the H/ACA small nucleolar ribonucleoprotein complex (H/ACA snoRNP), which consists of one unique H/ACA RNA and four common core proteins, Nhp2, Gar1, Nop10, and Cbf5 (Henras et al., 1998; Watkins and Bohnsack, 2012). H/ACA snoRNPs catalyze site-specific rRNA pseudouridylation guided by unique base-pairing between the guide sequence of H/ACA RNAs and substrate rRNA (Bousquet-Antonelli et al., 1997; Ganot et al., 1997; Ni et al., 1997; Ge and Yu, 2013). In this study, I examined the role of NHP2 in cyst formation and differentiation of GSC daughters during early oogenesis.

Materials and Methods

Flies

Flies were maintained on standard *Drosophila* medium at 25°C. The germline-specific Gal4 driver *nanos-Gal4*::*VP16 (nos-Gal4)* (Van Doren et al., 1998) was used to express the following UAS constructs: *UAS-Sxl*^{RNAi} (34393) and *UAS-NHP2*^{RNAi} (51784) from the Bloomington *Drosophila* Stock Center (BDSC), and *UASp-Flag-GFP-Sxl* and *UASp-Flag-GFP* (Ota et al., 2017). *Snf*^{148} (7398) was provided by BDSC. *NHP2-EGFP* and *UASp-NHP2* constructs were generated in this study (see following sections).

EGFP knock-in mediated by CRISPR/Cas9

The clustered regularly interspaced short palindromic repeat (CRISPR)/ CRISPR-associated endonuclease (Cas9) system was used to generate an EGFP knock-in allele of the *NHP2* locus by expressing an EGFP knock-in construct, Cas9, and guide RNA (gRNA) (Gokcezade et al., 2014). Using CRISPR Optimal Target Finder, the EGFP knock-in site was determined to be just upstream of the stop codon of the *NHP2* protein-coding region. The gRNA sequence encompassing the knock-in site was amplified using primer pair NHP2-EGFP-sgRNA-Fw/NHP2-EGFP-sgRNA-Rv (Table II-1), and cloned into *Bbs*I-digested pDCC6; this vector expresses gRNA and

Cas9 under the control of the U6-2 and *hsp70B* promoters, respectively (Gokcezade et al., 2014).

The EGFP knock-in construct contains the EGFP-coding sequence flanked by the 1-kb regions upstream and downstream of the *NHP2* stop codon. The EGFP coding sequence was amplified from pEGFP-N1 (Clontech) using primer pair pEGFP-N1-Fw/pEGFP-N1-Rv (Table II-1). The genomic regions upstream and downstream of the *NHP2* stop codon were amplified from genomic DNA of *y w* flies using primer pairs NHP2-upstream-1kb-Fw/NHP2-upstream-1kb-Rv and NHP2-downstream-1kb-Fw/NHP2-downstream-1kb-Rv (Table II-1), respectively. Using Gibson Assembly (New England BioLabs), the upstream, EGFP-coding, and downstream regions were assembled in pBluescript II SK(+) amplified using primer pair pBlue-Fw/pBlue-Rv (Table II-1). Approximately 0.1 nl of solution containing the *NHP2* knock-in construct and pDCC6 plasmid containing target sequences for *NHP2* (150 ng/μl each in distilled water) were injected into *y w* embryos. Progeny carrying the EGFP insertion at the *NHP2* target site was selected by PCR and used to establish stock lines.

Transgene

For construction of *UASp-NHP2*, the open reading flame (ORF) of *NHP2* was amplified from DNA clone RH66170 from the *Drosophila* Genomics Resource Center.

Primer pair “NHP2-RA-Fw/NHP2-RA-Rv” (Table II-1) was used to amplify the *NHP2* ORF. The *NHP2* ORF was then cloned into the *Kpn*I/*Not*I digested pUASp vector (Rørth, 1998). Germline transformation was performed using *y w* embryos as recipients. w^+ transformants were crossed to *w*; *Sp* / *CyO*; *PrDr* / *TM3* females to establish a homozygous stock of *UASp-NHP2*.

UV-crosslinked RNA immunoprecipitation (CLIP) and RT-qPCR

To perform CLIP analysis, ovaries were dissected from *nos-Gal4*, *nos-Gal4 UASp-EGFP,* and *nos-Gal4 UASp-Sxl-EGFP* flies. Twenty ovaries were homogenized in 10 µl of ice-cold buffer-A [8.3 mM KCl, 1.7 mM NaCl, 1 mM Tris/HCl (pH 7.5), cOmplete Protease Inhibitor Cocktail (Roche), and 100 U/ml RNasin Plus RNase Inhibitor (Promega)] and centrifuged at 20000 *g* for 10 min at 4°C. Five microliters of supernatant was mixed with 5 µl of binding buffer [BB: 200 mM KCl, 200 ng/µl yeast tRNA, 1 mg/ml heparin, 20 mM HEPES (pH 7.2), 6 mM $MgCl_2$, 2 mM DTT and 10% glycerol], irradiated using a CL-1000 Ultraviolet Crosslinker (UVP) at 17200 µJ/cm^2, and diluted to a final volume of 110 µl with PBST (PBS containing 0.1% TritonX-100 and 0.1% Tween20). RNAs were extracted using ISOGEN (NIPPON GENE) from 10 µl of the solution (representing 10% input). The remaining 100 µl of the solution was incubated with anti-GFP antibody (Thermo Fisher Scientific) in the presence of protein A–Sepharose beads (GE Healthcare) for 1 hr at 4°C. After incubation, beads were

precipitated and rinsed three times each with PBST and Pro-K buffer [0.01 M Tris-HCl (pH 7.8), 0.01 M EDTA, 0.5% SDS], and then incubated in the presence of 2 mg/ml protease K in Pro-K buffer for 20 min at 37°C. RNAs were extracted from the immunoprecipitate using ISOGEN. cDNAs were synthesized using SuperScript III (Thermo Fisher Scientific). *NHP2*, *nos*, *Tub84D,* and *rp49* were amplified using primer pairs NHP2-qPCR-Fw/NHP2-qPCR-Rv, nos-qPCR-Fw/nos-qPCR-Rv, Tub84D-qPCR-Fw/Tub84D-qPCR-Rv, and rp49-qPCR-Fw/rp49-qPCR-Rv (Table II-2), respectively. Quantification was performed on a Light Cycler 480 system (Roche) with the QuantiTect SYBR Green RT-PCR Kit (Qiagen). Thermal cycling conditions were as follows: 15 min at 95°C, followed by 55 cycles of 15 sec at 94°C, 30 sec at 60°C, and 20 sec at 72°C. Data were analyzed using the Light Cycler Software (Roche) and Microsoft Excel (Microsoft). Three independent experiments were carried out using different batches of flies.

The amounts of *NHP2-RA, NHP2-RB* (*RA/RB*), and *NHP2-RB* (*RB*) transcripts were determined using external standards identical to the target sequences. Standard curves for *NHP2-RA/RB* and *NHP2-RB* were generated using a dilution series of *Spe*I-digested pGEM-T easy vector (Promega) containing a sequence common to *NHP2-RA* and *RB* (*RA/RB*) or an *NHP2-RB*-specific (*RB*) cDNA fragment. Target sequences were amplified from cDNA synthesized from *bam* mutant ovaries using primer pairs NHP2-RARB-abs-qPCR-Fw/NHP2-RARB-abs-qPCR-Rv and

NHP2-RB-abs-qPCR-Fw/NHP2-RB-abs-qPCR-Rv (Table II-2). Quantification was performed using the Light Cycler 480 system and the QuantiTect SYBR Green RT-PCR Kit. Data were analyzed using the Light Cycler Software and Microsoft Excel. Absolute transcript levels were calculated by comparing the Cp values of *RA/RB* and *RB* transcripts with standard curves. Three independent experiments were carried out using different batches of flies.

Immunostaining

Immunofluorescence staining of adult ovaries was performed as described (Hayashi et al., 2004). Ovaries were dissected from adult flies 5–10 days after eclosion. The following primary antibodies were used at the indicated dilutions: mouse anti-Fibrillarin (1:500, Abcam), rabbit anti-GFP (1:500, Thermo Fisher Scientific), rabbit anti-Sxl (1:1000, a gift from Dr. Hiroshi Sakamoto), rabbit anti-Bam (1:1000), rabbit anti-active Caspase3 (1:1000, Abcam), chick anti-Vasa (1:500), mouse anti-Hts [1:10, 1B1; Developmental Studies Hybridoma Bank (DSHB)], and mouse anti-FasIII (1:10, 7G10 anti-FasciclinIII; DSHB). For detection of primary antibodies, the following secondary antibodies were used: Alexa Fluor 488–conjugated goat anti-rabbit (1:500, Molecular Probe), Alexa Fluor 546–conjugated goat anti-mouse (1:500, Molecular Probe), and Alexa Fluor 633–conjugated goat anti-chick (1:500, Molecular Probe). Samples were mounted in ProLong™ Diamond Antifade Mountant (Thermo

Fisher Scientific) and observed by confocal microscopy SP5 (Leica Microsystems).

In situ hybridization

Whole-mount *in situ* hybridization of adult gonads was performed as described (Hayashi et al., 2004). Total RNA was isolated from ovaries using ISOGEN, and cDNA was synthesized using SuperScript III. cDNA corresponding to *NHP2* was PCR-amplified using primer pair NHP2-FISH-Fw/NHP2-FISH-Rv (Table II-1). The resultant cDNA amplicon was cloned into pGEM-T Easy (Promega). Digoxigenin (DIG)-labeled RNA probes were synthesized with T7 or SP6 RNA polymerase (Roche) using the fragment amplified from the plasmid using the T7 and SP6 primers. Signal was detected using horseradish peroxidase–conjugated anti-DIG antibody (Roche) and amplified using the TSA Biotin System and streptavidin–fluorescein (FITC, PerkinElmer). *In situ* hybridization combined with immunostaining was performed as described (Hayashi et al., 2004). Ovaries were stained with chick anti-Vasa, mouse anti-Hts, and mouse anti-FasIII antibodies. Secondary antibodies were Alexa Fluor 546–conjugated goat anti-rabbit and Alexa Fluor 633–conjugated goat anti-chick.

OPP staining

OPP staining was performed using the Click-iT Plus OPP Alexa Fluor 488 Protein Synthesis Assay Kit (Molecular Probes). Ovaries were dissected in Grace’s

insect medium (Thermo Fisher Scientific) from adult flies 5–10 days after eclosion. The ovaries were incubated in 20 μM Click-iT OPP reagent in Grace's insect medium for 30 min at room temperature. After incubation, ovaries were fixed in 4% paraformaldehyde in PBS for 20 min, and then washed with PBS containing 0.1% Tween-20 and 0.1% Triton X-100 (PBT) three times for 20 min each. For the Click-iT reaction, ovaries were incubated in Click-iT reaction cocktail in the dark at room temperature. After 30 min, ovaries were washed with Click-iT reaction rinse buffer. Ovaries were then washed with PBT three times for 20 min each and immunostained as described above.

Results and Discussion

Expression of *NHP2* mRNA and its protein product during cyst formation

The *NHP2* locus encodes two mRNA isoforms, which contain identical protein-coding regions (Fig. II-1B) (FlyBase: www.flybase.org). To examine the expression of *NHP2* mRNA during cyst formation, I performed fluorescence *in situ* hybridization (FISH) of ovaries using a probe capable of detecting both mRNA isoforms (Fig. II-1B; green line). The signal for *NHP2* mRNA was almost evenly distributed throughout the cytoplasm of the germline during cyst formation from single cells to 8-cell cysts in region 1 (R1), and was increased in disc-shaped 16-cell cysts surrounded by follicle cells in region 2 (R2) (Fig. II-1C–C′′, D, D′, E and E′). Next, I examined expression of NHP2 protein during cyst formation. Because I was unable to raise an antibody against NHP2 protein, I inserted a tag sequence encoding an enhanced green fluorescent protein (EGFP) into the C-terminus of the *NHP2* coding region (*NHP2-EGFP*) (Gokcezade et al., 2014), enabling me to detect NHP2 protein using an anti-GFP antibody. I found that NHP2-EGFP accumulated in nuclei of germline cells during cyst formation (Fig. II-2A–A′′). In their nuclei, NHP2-EGFP was enriched in a region stained by an antibody against Fibrillarin, a component of the nucleolus (Fig. II-2B–B′′, C–C′′ and D–D′′), indicating that NHP2-EGFP was concentrated in the nucleoli of germline cells during cyst formation. This is consistent with the fact that the

yeast ortholog, Nhp2, is a component of the H/ACA-box small nucleolar RNAs and protein complex (H/ACA snoRNPs), which guides pseudouridylation of rRNA in the nucleolus (Henras et al., 1998; Maiorano et al., 1999; Pogacic et al., 2000; Kierzek et al., 2014).

Changes in NHP2-EGFP expression and nucleolar morphology were evident in the germline during cyst formation (Fig. II-2B–D, B′–D′ and B′′–D′′) (Sanchez et al., 2016). Single cells and 2-, 4-, 8-, and 16-cell cysts can be distinguished by counting the number of germline cells interconnected by branched fusomes (Fig. II-1A). In single cells and 2-cell cysts in R1 of the germarium, I observed large nucleoli marked by NHP2-EGFP (Fig. II-2E, E′, F and F′). When these germline cells progressed to 4- and 8-cell cysts in R1, NHP2-EGFP staining was significantly reduced (Fig. II-2G, G′, H and H′), and nucleolar size was decreased (Fig. II-2C′′). Although NHP2-EGFP staining remained at a low level in newly formed 16-cell cysts (Fig. II-2I and I′), in disc-shaped 16-cell cysts in R2, staining increased (Fig. II-2J and J′), and the nucleoli were expanded (Fig. II-2D′′). These observations demonstrate that abrupt downregulation of NHP2 expression occurs during progression from 2-cell to 4-cell cysts.

Germline-specific knockdown (GS-KD) of *NHP2* promotes progression to 8-cell cysts

NHP2 GS-KD causes a defect in egg-chamber formation (Sanchez et al., 2016). NHP2 function is required in GSCs for complete cytokinesis, and reduction in the level of this protein results in formation of interconnected undifferentiated cells, or stem cysts (Sanchez et al., 2016). Consistent with this, *NHP2* GS-KD impaired 16-cell cyst formation (Fig. II-3A, A′, B, B′ and C). Moreover, the numbers of single cells were drastically reduced in *NHP2* GS-KD germarium, and the numbers of 4- and 8-cell cysts were elevated, in comparison with *nos-Gal4* (Fig. II-3C). This suggests that NHP2 is required to maintain single cells, and that NHP2 downregulation initiates progression to 4- and 8-cell cysts. Next, I asked whether accumulation of 4- and 8-cell cysts in the *NHP2* GS-KD germarium results from progression of cyst formation, or merely from disruption of cytokinesis between undifferentiated germline stem cells (GSCs) (single cells). Knockdowns of translation initiation factors and ribosomal assembly factors cause formation of abnormal cysts (stem cysts) containing Bam-negative undifferentiated germline cells connected with each other by branched fusomes in the germaria (Sanchez et al., 2016). Furthermore, stem cysts exhibit nucleolar hypertrophy, a characteristic of single cells and 2-cell cysts (Sanchez et al., 2016).

Similar to 4- and 8-cell cysts in normal germaria, I found that 4- and 8-cell cysts in *NHP2* GS-KD germaria expressed high levels of Bam protein (Bam-positive 4-

and 8-cell cysts) (Fig. II-4A–A′′ and B–B′′). The number of Bam-positive 8-cell cysts was significantly higher in *NHP2* GS-KD than in *nos-Gal4* germaria (Table II-3), although there was no significant difference in the number of Bam-positive 4-cell cysts between *NHP2* GS-KD and *nos-Gal4* germaria. Furthermore, Bam-positive 4- and 8-cell cysts in *NHP2* GS-KD germaria did not exhibit nucleolar hypertrophy (Fig. II-4C–C′′ and D–D′′). These observations suggest that *NHP2* GS-KD promotes proper differentiation to 8-cell cysts, which retain proper cell identity as evidenced by high levels of Bam expression and smaller nucleolar size. However, differentiation into 16-cell cysts appeared to be arrested in *NHP2* GS-KD germaria (Fig. II-3C), and some of these cysts may have eventually been eliminated by apoptosis (Fig. II-5A, A′, B, B′ and C).

On the other hand, 4- and 8-cell cysts with undetectable or low levels of Bam expression (Bam-negative 4- and 8-cell cysts) were frequently observed in the proximity of the distal tips of germaria, where niche cells reside. These Bam-negative cysts were regarded as "stem cysts" (Fig. II-4B–B′′, D–D′′, Table 1). This observation suggests that stem cysts were also formed in *NHP2* GS-KD germaria. Thus, proper progression of cyst formation, along with abnormal stem-cyst formation, results in the accumulation of 4- and 8-cell cysts in *NHP2* GS-KD germaria.

NHP2 GS-KD partially rescues the defect caused by *Sxl* GS-KD in cyst formation

The data presented above indicate that downregulation of *NHP2* facilitates progression to 8-cell cysts. This is compatible with the observation that expression of NHP2 protein is decreased in 4- and 8-cell cysts compared with single and 2-cell cysts (Fig. II-2E′–H′). I speculate that downregulation of the NHP2 protein promotes progression from 2- to 8-cell cysts through 4-cell cysts. Because *NHP2* mRNA was almost evenly detected throughout cyst formation until 8-cell cysts (Fig. II-1D, D′, E and E′), it is reasonable to speculate that NHP2 protein production is repressed at a post-transcriptional level in 4- and 8-cell cysts. The strongest candidate for the gene responsible for downregulating NHP2 during cyst formation is *Sex lethal* (*Sxl*). Reduction in *Sxl* activity causes a tumorous phenotype, which is characterized by accumulation of single cells and 2-cell cysts in germaria (Fig. II-6A, A′ and C) (Steinmann-Zwicky et al., 1989). *Sxl* GS-KD caused a reduction in the numbers of 4-, 8-, and 16-cell cysts (Fig. II-6A, A’ and C). The defects caused by *Sxl* GS-KD were partially rescued by introduction of *NHP2* GS-KD (Fig. II-6B, B′ and C). When *Sxl* and *NHP2* activities were concomitantly repressed (*NHP2-Sxl* GS-KD), the tumorous phenotype was suppressed, and the numbers of 4- and 8-cell cysts were increased (Fig. II-6B, B′ and C).

I next asked whether these 4- and 8-cell cysts properly express high levels of Bam protein, as is the case for normal cyst formation. In *Sxl* GS-KD germaria, the

accumulating single cells and 2-cell cysts exhibited modest levels of Bam expression (Fig. II-6D–D′′) (Chau et al., 2009). Because Bam expression is undetectable or low in these cells in normal germaria (Fig. II-4A–A′′) (McKearin and Spradling, 1990; McKearin and Ohlstein, 1995; Chen and McKearin, 2003b;), single cells and 2-cell cysts may partially adopt 4- and 8-cell cyst identity in *Sxl* GS-KD. However, I found that 4- and 8-cell cysts expressed Bam in *NHP2-Sxl* GS-KD at a much higher level than in single cells and 2-cell cysts in *Sxl* GS-KD (Fig. II-6D–D′′ and E–E′′). There was a statistically significant increase in the number of Bam-positive 8-cell cysts in *NHP2-Sxl* GS-KD germaria in comparison with those of *Sxl* GS-KD, but no significant difference between *NHP2-Sxl* and *Sxl* GS-KD in the number of Bam-positive 4-cell cysts (Table II-4). These data suggest that single cells and 2-cell cysts in *Sxl* GS-KD can progress properly to 8-cell cysts by introduction of *NHP2* GS-KD. Based on these findings, it is reasonable to conclude that *Sxl* represses *NHP2* activity to promote proper cyst formation. However, 16-cell cysts were rarely observed in either *NHP2* GS-KD or *NHP2-Sxl* GS-KD germaria (Fig. II-3C and II-5C). This suggests that *NHP2* activity is also required to promote progression from 8- to 16-cell cysts.

Sxl protein binds to *NHP2* mRNA during cyst formation

Sxl encodes an RNA-binding protein that regulates sex-biased translation and splicing of target mRNAs (Penalva and Sánchez, 2003). In the soma, *Sxl* is expressed in

embryos in a female-specific manner (Bopp et al., 1991; Keyes et al., 1992). Sxl protein regulates alternative splicing of *transformer* (*tra*) RNA to produce functional Tra protein only in female soma. Furthermore, Sxl protein binds to 5′ and 3′ untranslated regions (UTRs) of *male-specific lethal 2* (*msl2*) RNA in female soma to repress its translation (Bashaw and Baker, 1997; Kelly et al., 1997; Beckmann et al., 2005; Lucchesi and Kuroda, 2015). Considering the molecular function of Sxl protein in the soma, I speculate that Sxl binds to *NHP2* mRNA and represses its translation in 4- and 8-cell cysts in germaria.

NHP2 mRNA co-immunoprecipitates with Sxl-enhanced green fluorescent protein (EGFP) fusion protein in primordial germ cells and contains a Sxl-binding motif (Fig. II-1B) (Ota et al., 2017). The Sxl-binding motif is located at the 3′ UTR of *NHP2-RB*, but not in *NHP2-RA* 3′ UTR (Fig. II-1B). I observed *NHP2-RB* expression in single cells and 2-cell cysts in *bam* mutant ovaries (Fig. II-7A), but I could not determine whether *NHP2-RB* was expressed in 4- and 8-cell cysts in normal germaria because the *RB*-specific probe (116 bp) is too short to detect *NHP2-RB* expression by *in situ* hybridization.

To determine whether Sxl protein binds to *NHP2-RB* 3′ UTR during cyst formation, I performed UV-crosslinked RNA immunoprecipitation (CLIP). Extracts prepared from ovaries expressing Sxl-EGFP and EGFP in the germline were immunoprecipitated with an anti-GFP antibody, and *NHP2-RB* 3′ UTR was detected by

RT-qPCR using a primer set amplifying the 3′ UTR region encompassing the Sxl-binding motif. As a positive control, I examined the precipitation of *nos* mRNA, whose 3′ UTR contains a Sxl-binding motif and binds Sxl protein (Chau et al., 2012). *NHP2-RB* and *nos* 3′ UTRs were more abundant in immunoprecipitate from Sxl-EGFP-expressing ovaries (Sxl-EGFP IP) than from EGFP-expressing ovaries (EGFP IP) (Fig. II-7B). By contrast, *Tub84D* and *rp49*, which contain no Sxl-binding motif in their 3′ UTRs, were not enriched in Sxl-EGFP IP in comparison with EGFP IP (Fig. II-7B). These results strongly suggest that Sxl protein binds to the *NHP2-RB* 3′ UTR in the ovarian germline.

Sxl protein accumulates in GSCs (Chau et al., 2009), but its expression during cyst formation remains unclear. I found that Sxl protein was highly expressed in single cells and 2- and 4-cell cysts (Fig. II-8A–A′′ and B–B′′), but its expression was gradually reduced in 8-cell cysts (Fig. II-8C–C′′) and 16-cell cysts (Fig. II-8A–A′′, B–B” and C–C′′). Thus, Sxl was expressed in 4- and 8-cell cysts, in which expression of NHP2 protein was reduced. By contrast, in single cells and 2-cell cysts, both Sxl and NHP2 were highly expressed. Therefore, I speculate that Sxl requires a corepressor to suppress NHP2 production in 4- and 8-cell cysts, and that its expression is restricted in these cysts. Sxl acts with a corepressor to suppress translation of *msl-2* mRNA in the soma (Duncan et al., 2006; Duncan et al., 2009).

In Fig. II-7A, I show that *NHP2-RB* constitutes approximately 30% of the

total expression level of *NHP2* mRNA in *bam* mutant ovaries. Although I cannot exclude the possibility that *NHP2-RB* is a major variant of *NHP2* mRNA in 4-cell and 8-cell cysts, I speculate that Sxl-dependent translational repression of the *NHP2-RB* variant causes a reduction in NHP2 protein expression in 4- and 8-cell cysts. My data suggest that this downregulation of NHP2 protein facilitates progression from 2-cell cysts to 4- and 8-cell cysts. If this is the case, one would expect that germline-specific overexpression of *NHP2* (*NHP2* GS-OE) causes a tumorous phenotype characterized by the accumulation of single cells and 2-cell cysts in the germarium, such as that observed in *Sxl* GS-KD. Indeed, *NHP2* GS-OE caused a statistically significant but modest increase in the number of single cells and 2-cell cysts in the germarium (Fig. II-9). However, 4- to 16-cell cysts were still observed in the *NHP2* GS-OE germarium (Fig. II-9). These data suggest that *NHP2* GS-OE is insufficient to cause the tumorous phenotype. This can be explained by the idea that NHP2 requires co-factors to execute its function in cyst formation. NHP2 co-factor(s) may be active in single cells and 2-cell cysts, but may be inactivated by Sxl in 4- and 8-cell cysts. Thus, *NHP2* GS-KD is able to eliminate NHP2 function in single cells and 2-cell cysts, but *NHP2* GS-OE is unable to upregulate NHP2 function in 4- and 8-cell cysts.

Proper regulation of pseudouridylation is required for progression of cyst formation

The observations described above support the idea that progression to 4- and 8-cell cysts requires downregulation of NHP2 expression, and that NHP2 is suppressed at the translational level in 4- and 8-cell cysts by Sxl function.

The genes required for GSC differentiation are repressed by *nanos* (*nos*). Once the daughter cells of asymmetric GSC divisions detach from the niche, Sxl becomes active and represses Nos expression at a translational level, collaborating with Benign gonial cell neoplasia (Bgcn), Mei-P26, and Bam proteins; expression of all of these factors is repressed by Dpp signaling from the niche (Chen and McKearin, 2003b; Song et al., 2004; Li et al., 2009; Chau et al., 2012; Li et al., 2013). Thus, Sxl enables the switch from the GSC to differentiating state by suppressing *nos* translation (Slaidina and Lehmann, 2014). By analogy, I speculate that Sxl plays an additional role in progression of cyst formation by suppressing NHP2 production. Of course, I cannot rule out the alternative possibility that accumulation of Bam-positive 4- and 8-cell cysts in *NHP2* GS-KD and *NHP2-Sxl* GS-KD germaria resulted from de-repression of Bam in the stem cysts, which are separated from the niche. To address this issue, further work is necessary to examine whether 4- and 8-cell cysts have gene expression profiles similar to those of normally developing cysts.

It remains to be determined how NHP2 modulates cyst formation.

Knockdowns of genes involved in ribosome assembly, including H/ACA snoRNP complex, impair GSC differentiation and cause formation of stem cysts. Moreover, knockdowns of genes encoding ribosomal subunits and rRNA transcription induce a GSC loss phenotype (Sanchez et al., 2016). Furthermore, 4- and 8-cell cysts accumulate in *bam* mutant germaria when mutations are introduced in either *pelota* (which encodes a translational release factor–like protein) or *under-developed* (which encodes an RNA polymerase I cofactor) (Xi, 2005; Zhang et al., 2014). Thus, it is reasonable to assume that modulation of translational activity is essential for GSC differentiation and cyst formation. However, I found that global protein synthesis, monitored by O-propargyl-puromycin and L-homopropargylglycine Click-iT staining (OPP staining) (Liu et al., 2012), did not decrease in 4- and 8-cell cysts, in which NHP2 expression was downregulated (Fig. II-10A–A′′) (Sanchez et al., 2016), and *NHP2* GS-KD did not affect OPP staining in germarium (Fig. II-10B–B′′). Thus, I speculate that NHP2-dependent pseudouridylation, rather than global translation activity, must be precisely regulated to promote proper cyst formation.

Alteration in pseudouridylation of rRNA causes a defect in translation of specific mRNAs containing IRES (internal ribosome entry site) in yeast, mouse, and human (Yoon et al., 2006; Gilbert, 2011; Jack et al., 2011; Xue and Barna, 2012). Furthermore, in *Xenopus* embryos and human embryonic stem cells, a complex containing NHP2 and RNA Polymerase I induces neural crest specification by altering

translation of specific mRNAs without affecting global translation activity (Werner et al., 2015). Therefore, it is possible that reduction in rRNA pseudouridylation alters translation of specific mRNAs, which in turn promotes progression of cyst formation. Further studies are needed to identify the mRNAs whose translation is altered by *NHP2* GS-KD, and to examine their roles in the progression of cyst formation.

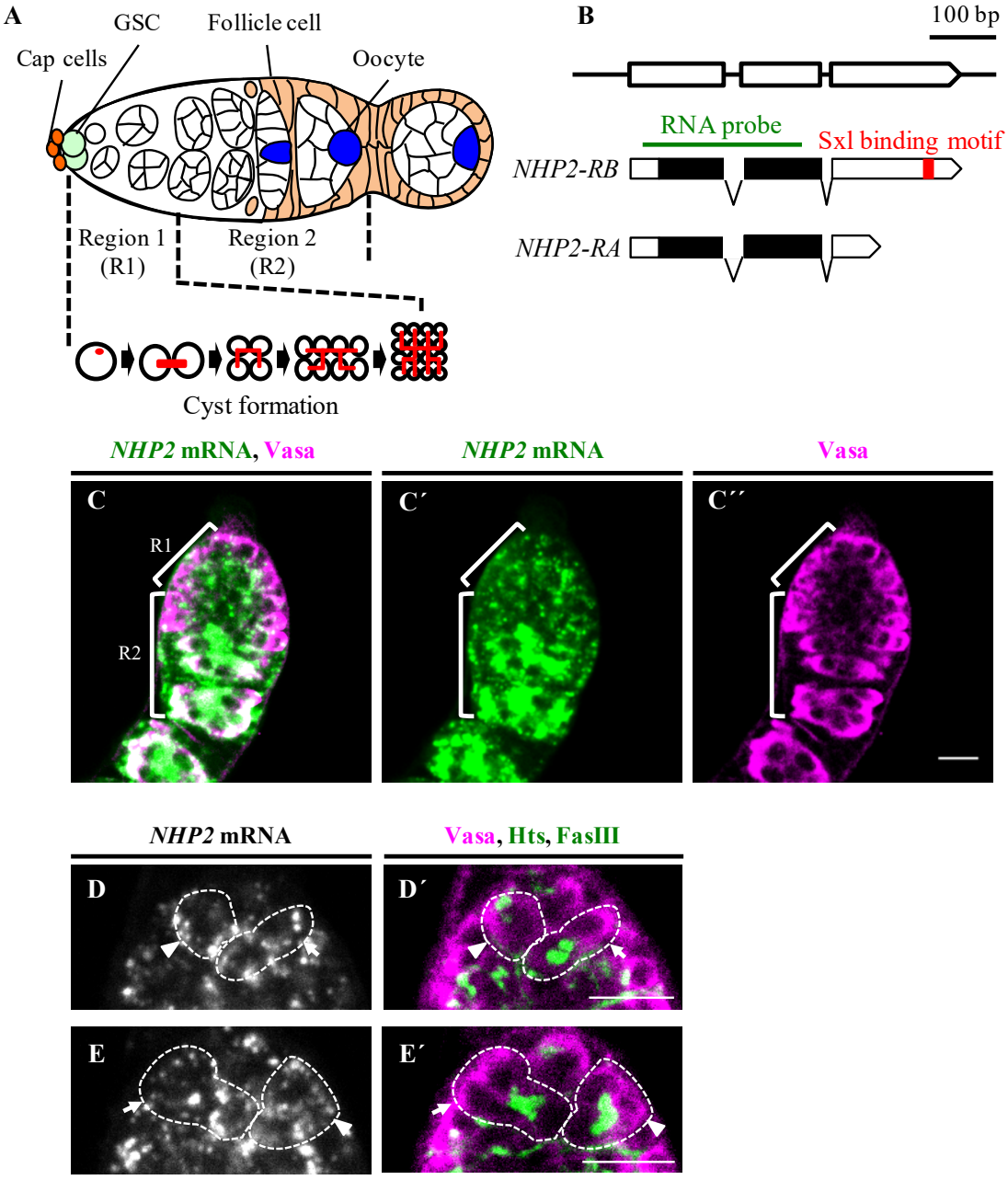
A
GSC
Follicle cell
Cap cells
Oocyte
Region 1
(R1)
Region 2
(R2)
Cyst formation
B
100 bp
RNA probe
Sxl binding motif
NHP2-RB
NHP2-RA
NHP2 mRNA, Vasa
NHP2 mRNA
Vasa
C
C´
C´´
R1
R2
NHP2 mRNA
Vasa, Hts, FasIII
D
D´
E
E´

Fig. II-1. Expression of *NHP2* mRNA in germarium.

(A) Schematic diagram of *Drosophila* germarium. GSCs (light green) adhere to cap cells (orange) located at the distal tip of the germarium. In region 1 (R1), a GSC divides to produce two daughter cells: one remains as a GSC, whereas the other (cystoblast) differentiates. In this article, the GSC and cystoblast are referred to as single cells. Cystoblast undergoes four synchronous mitotic division with incomplete cytokinesis (cyst formation) to form 2-, 4-, 8-, and 16-cell cysts interconnected by the fusome (red), a derivative of the spectrosome (red) in the single cell. In region 2 (R2), among the 16 cells, one differentiates into an oocyte (blue) and remaining 15 cells become nurse cells. Oocyte and nurse cells are encapsulated by a monolayer of follicle cells (light brown). (B) *NHP2* encodes two mRNA variants, *NHP2-RA* and *NHP2-RB*. Exons (boxes), introns (straight lines), protein-coding regions (black boxes), Sxl-binding motif (red), and the region detected by the RNA probe (green line) are shown. (C–C′′) *nos-Gal4* germarium *in situ* hybridized with an RNA probe for *NHP2* (green in C and C′) and immunostained for Vasa, a marker of germline cells (magenta in C and C′′). White brackets indicate R1 and R2. Scale bar: 10 μm. (D, D′, E and E′) *nos-Gal4* germarium stained for *NHP2* mRNA (gray in D and E); Hts, a marker of spectrosomes and fusomes; FasIII, a marker of a subset of somatic cells including follicle cells (green in D’ and E’); and Vasa (magenta in D′ and E′). Single cells (arrowheads in D and D′), 2-cell cysts (arrows in D and D′), 4-cell cysts (arrowheads in E and E′), and 8-cell cysts (arrows in E and E′) are indicated by white dotted circles. Scale bars: 10 μm.

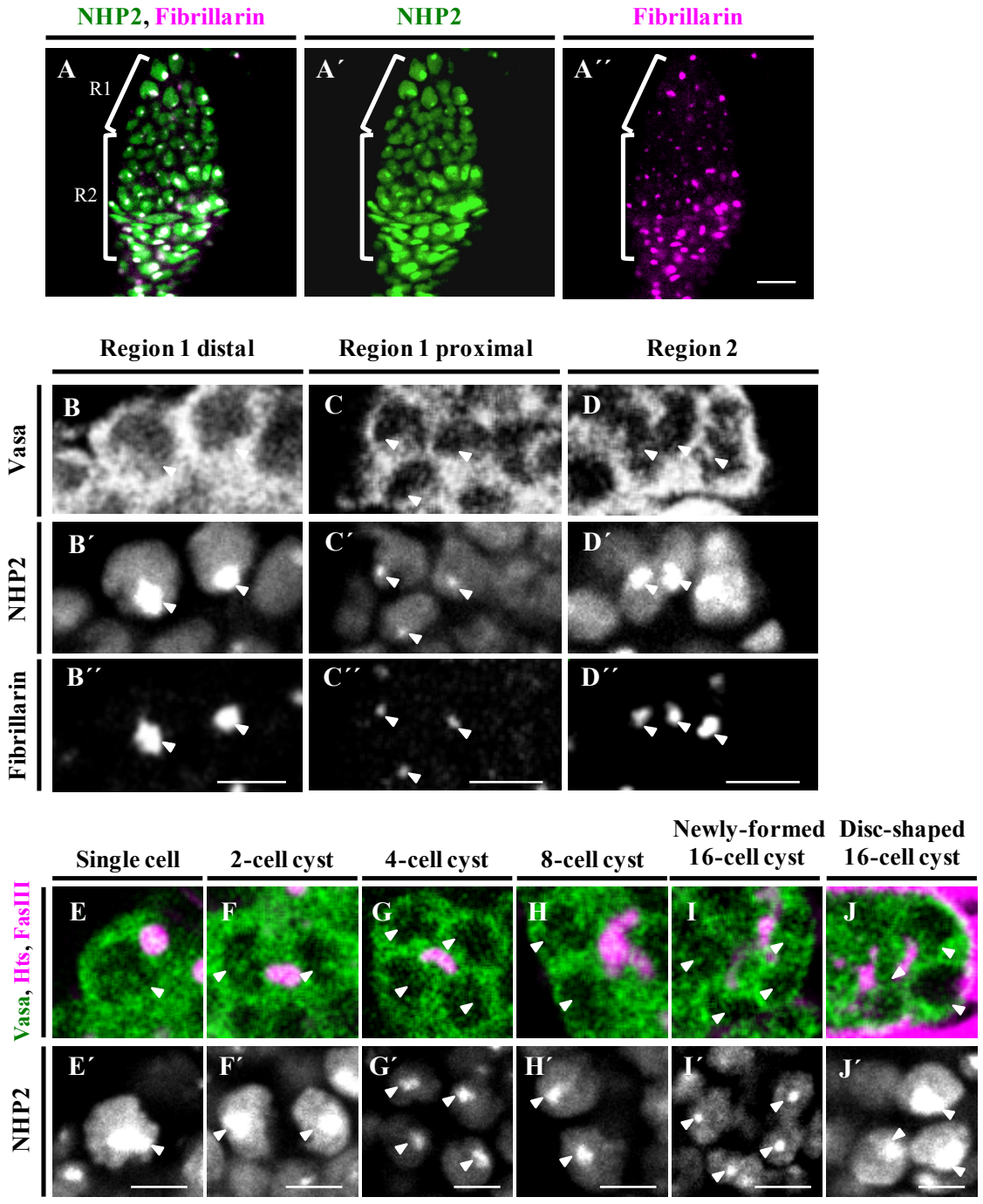
NHP2, Fibrillarin
NHP2
Fibrillarin
A
R1
R2
A´
A´´
Region 1 distal
Region 1 proximal
Region 2
Vasa
NHP2
Fibrillarin
B
C
D
B´
C´
D´
B´´
C´´
D´´
Single cell
2-cell cyst
4-cell cyst
8-cell cyst
Newly-formed 16-cell cyst
Disc-shaped 16-cell cyst
Vasa, Hts, FasIII
NHP2
E
F
G
H
I
J
E´
F´
G´
H´
I´
J´

Fig. II-2. Expression of NHP2 protein in germarium.

(A–A′′) *NHP2-EGFP* germarium immunostained for EGFP (green in A and A′) and Fibrillarin, a marker of nucleoli (magenta in A and A′′). Scale bar: 10 μm. (B–B′′, C–C′′ and D–D′′) Distal part of R1 (B–B′′), proximal part of R1 (C–C′′), and R2 (D–D′′) in *NHP2-EGFP* germaria immunostained for Vasa (upper panels), EGFP (middle panels), and Fibrillarin (lower panels). White arrowheads indicate nucleoli in the germline nuclei. Scale bars: 5 μm. (E–J and E′–J′) *NHP2-EGFP* germaria immunostained for Vasa (green in E–J), Hts and FasIII (magenta in E–J), and EGFP (gray in E′–J′). Single cells (E and E′), 2-cell cysts (F and F′), 4-cell cysts (G and G′), 8-cell cysts (H and H′), newly formed 16-cell cysts (I and I′), and disc-shaped 16-cell cysts (J and J′) are shown. White arrowheads indicate NHP2-EGFP foci in germline nuclei. Scale bars: 5 μm.

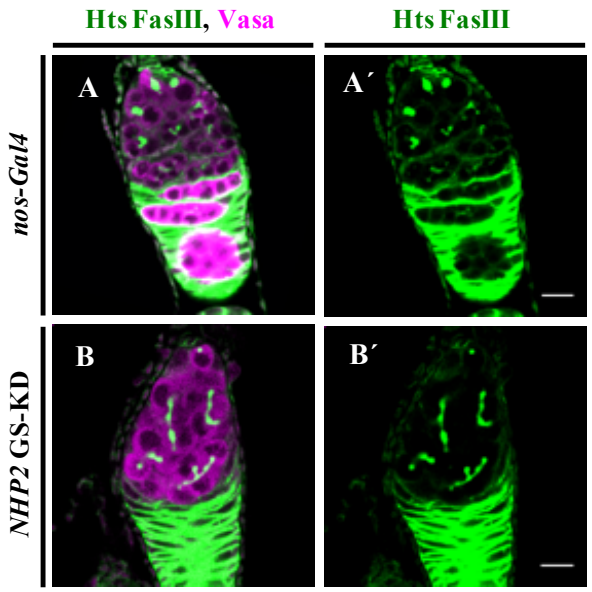
Hts FasIII, Vasa
Hts FasIII
nos-Gal4
NHP2 GS-KD
A
A´
B
B´

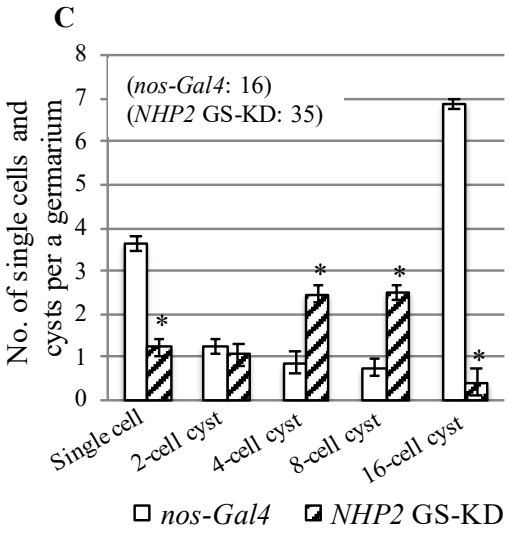
C
(nos-Gal4: 16)
(NHP2 GS-KD: 35)
No. of single cells and cysts per a germarium
0
1
2
3
4
5
6
7
8
Single cell
2-cell cyst
4-cell cyst
8-cell cyst
16-cell cyst
nos-Gal4
NHP2 GS-KD

Fig. II-3. Defects in cyst formation in *NHP2* GS-KD germarium.
(A, A′, B and B′) *nos-Gal4* (A and A′) and *NHP2* GS-KD germarium (B and B′) immunostained for Hts and FasIII (green) and Vasa (magenta in A and B). Scale bars: 10 μm. (C) Average numbers of single cells and 2-, 4-, 8-, and 16-cell cysts per a germarium from *nos-Gal4* (open bars) and *NHP2* GS-KD females (hatched bars) are indicated. Error bars indicate standard error. Significance of the difference relative to *nos-Gal4* was calculated by Student's t-test (* $P < 0.05$). The number of germaria examined is shown in parentheses.

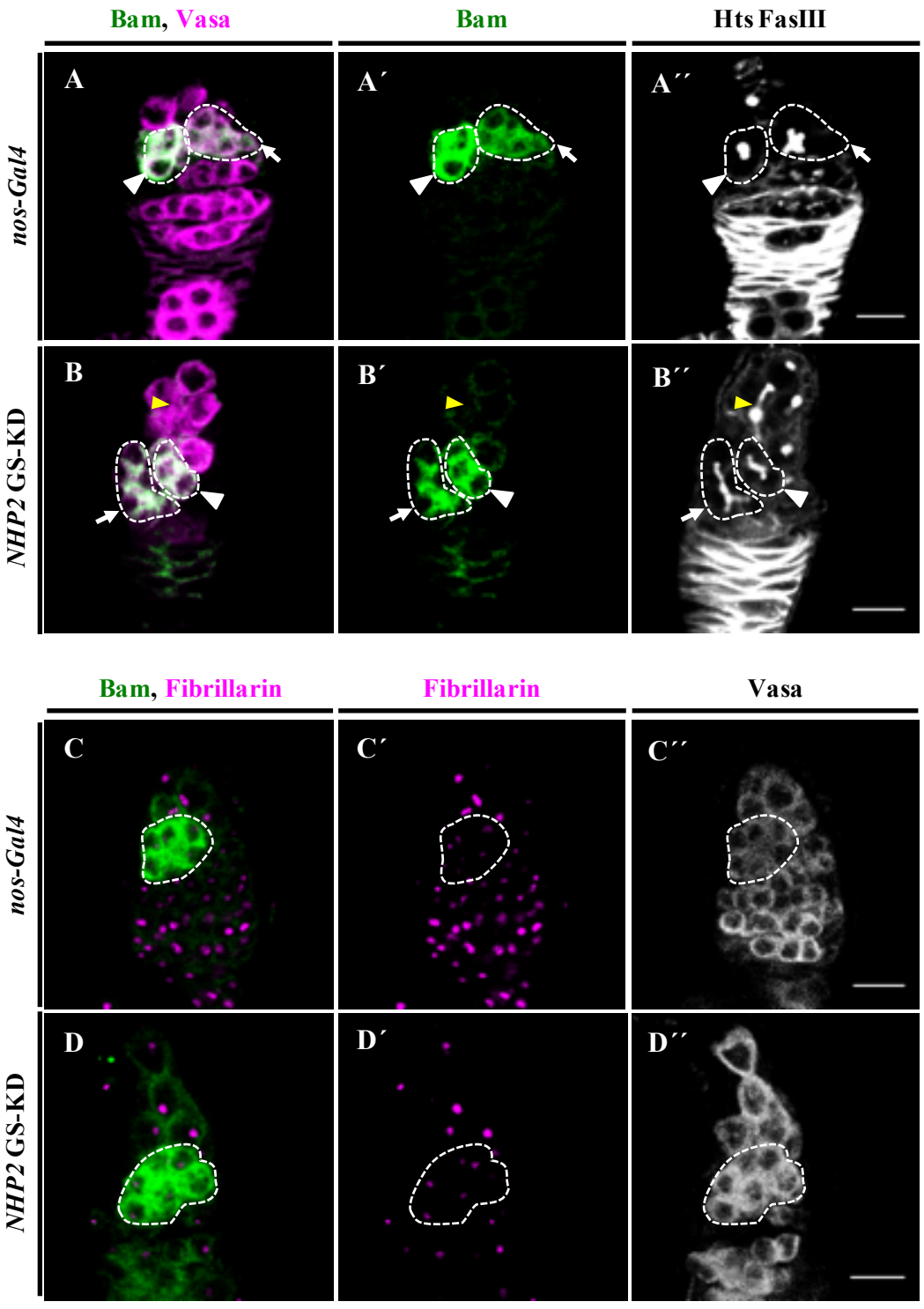
Bam, Vasa
Bam
Hts FasIII
A
A′
A′′
nos-Gal4
B
B′
B′′
NHP2 GS-KD
Bam, Fibrillarin
Fibrillarin
Vasa
C
C′
C′′
nos-Gal4
D
D′
D′′
NHP2 GS-KD

Fig. II-4. Expression of Bam in 4- and 8-cell cyst of *NHP2* GS-KD germarium. (A–A′′ and B–B′′) *nos-Gal4* (A–A′′) and *NHP2* GS-KD germarium (B–B′′) immunostained for Bam (green in A, A′, B and B′), Hts and FasIII (gray in A′′ and B′′), and Vasa (magenta in A and B). White dotted circles indicate 4-cell cysts (arrowheads) and 8-cell cysts (arrows). Yellow arrowheads indicate Bam-negative 4-cell cyst. Scale bars: 10 μm. (C–C′′ and D–D′′) *nos-Gal4* (C–C′′) and *NHP2* GS-KD germarium (D–D′′) immunostained for Bam (green in A and B), Fibrillarin (magenta in C, C′, D and D′), and Vasa (gray in C′′ and D′′). Bam-positive cysts are indicated by white dotted circles. In D–D′′, the germline cells above the Bam-positive cyst expressed low levels of Bam and showed nucleolar hypertrophy. These cysts are regarded as "Bam-negative cysts" (see text), and are classified as "stem cysts" based on their weak Bam expression and nucleolar morphology. Scale bars: 10 μm.

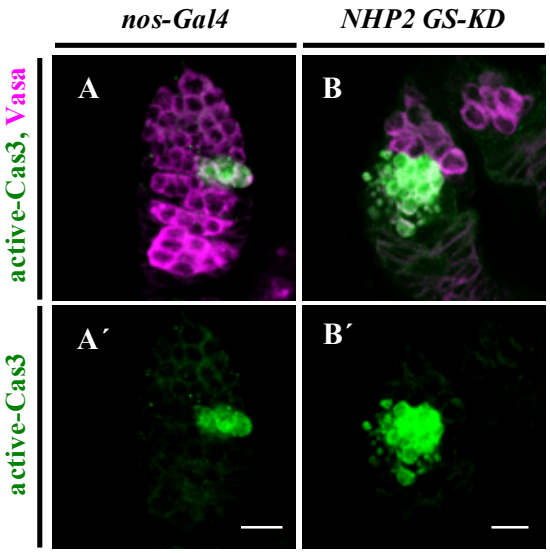
nos-Gal4
NHP2 GS-KD
active-Cas3, Vasa
active-Cas3
A
B
A´
B´

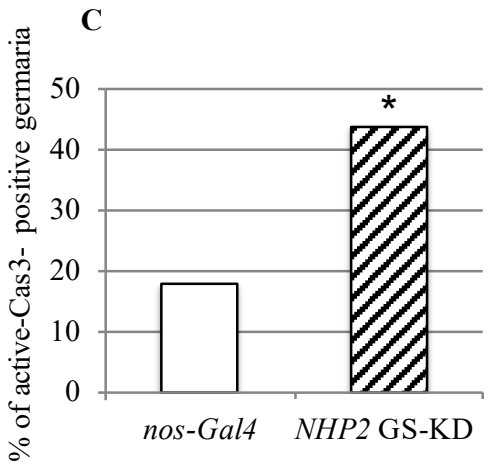
C
% of active-Cas3- positive germaria
50
40
30
20
10
0
*
nos-Gal4
NHP2 GS-KD

Figure II-5. Apoptosis in *NHP2* GS-KD germarium.

(A, A′, B, and B′) *nos-Gal4* (A and A′) and *NHP2* GS-KD germarium (B and B′) immunostained for active Caspase3 (Cas3), a marker of apoptotic cell death (green), and Vasa (magenta in A and B). Scale bars: 10 μm. (C) Percentages of active Cas3–positive germaria in *nos-Gal4* (open bar) and *NHP2* GS-KD ovaries (hatched bar). A total of 72 (*nos-Gal4*) and 89 (*NHP2* GS-KD) germaria were counted. Significance of the difference relative to *nos-Gal4* was calculated by Fisher's exact test (* $P < 0.01$).

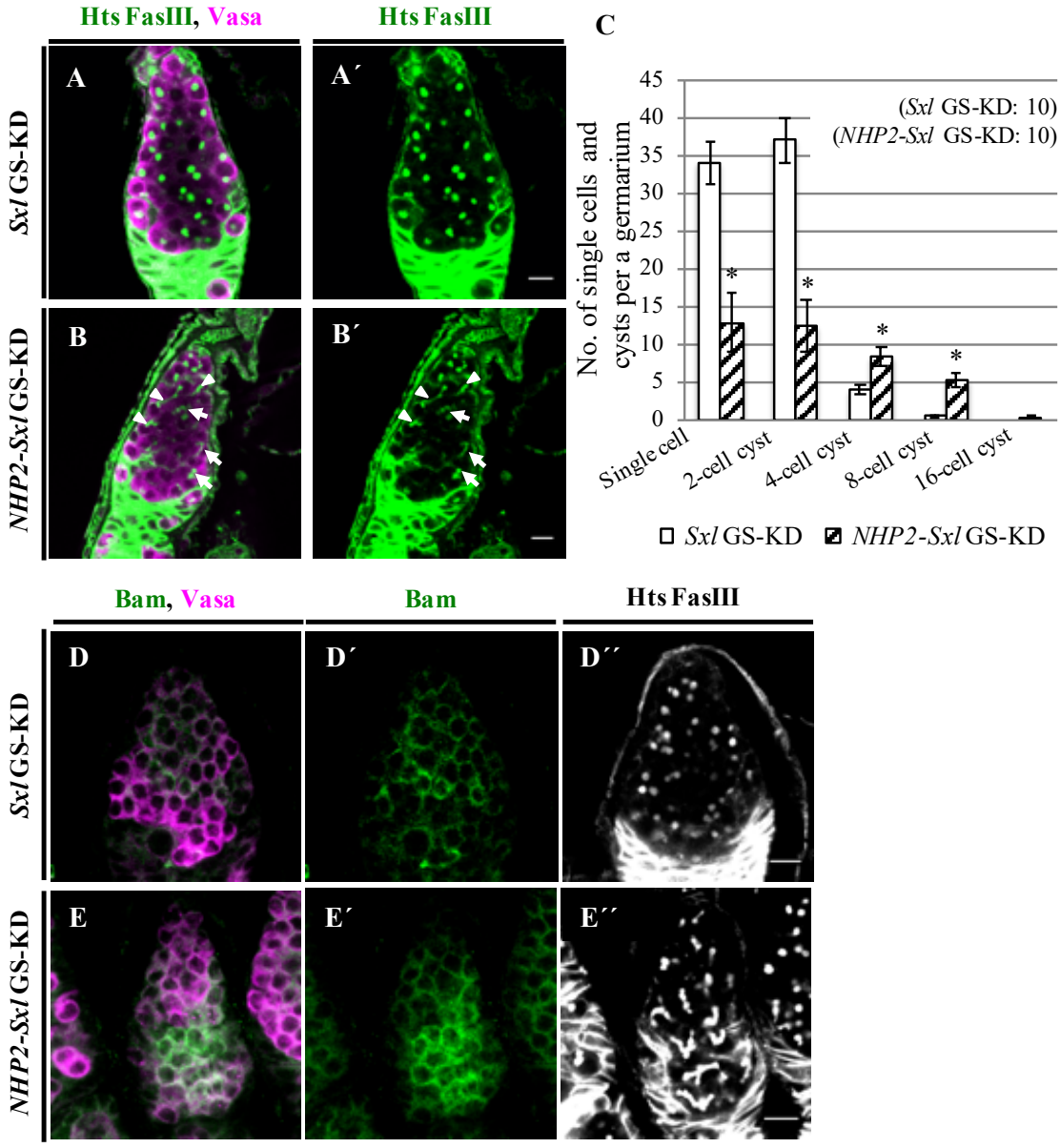
Hts FasIII, Vasa
Hts FasIII
A
A´
B
B´
Sxl GS-KD
NHP2-Sxl GS-KD
C
No. of single cells and cysts per a germarium
45
40
35
30
25
20
15
10
5
0
(Sxl GS-KD: 10)
(NHP2-Sxl GS-KD: 10)
*
Single cell
2-cell cyst
4-cell cyst
8-cell cyst
16-cell cyst
Sxl GS-KD
NHP2-Sxl GS-KD
Bam, Vasa
Bam
Hts FasIII
D
D´
D´´
E
E´
E´´
Sxl GS-KD
NHP2-Sxl GS-KD

Fig. II-6. Defects in cyst formation in *NHP2-Sxl* GS-KD germarium.
(A, A′, B and B′) *Sxl* GS-KD (A and A′) and *NHP2-Sxl* GS-KD germarium (B and B′) immunostained for Hts and FasIII (green) and Vasa (magenta in A and B). Arrows and arrowheads indicate 4- and 8-cell cysts respectively. Scale bars: 10 μm. (C) Average numbers of single cells and 2-, 4-, 8-, and 16-cell cysts per a germarium from *Sxl* GS-KD (open bars) and *NHP2-Sxl* GS-KD females (hatched bars) are indicated. Error bars indicate standard error. Significance of the difference related to *Sxl* GS-KD was calculated by Student's t-test (* $P < 0.05$). The number of germaria examined is shown in parentheses. (D–D′′ and E–E′′) *Sxl* GS-KD (D–D′′) and *NHP2-Sxl* GS-KD germarium (E–E′′) immunostained for Bam (green in D, D′, E and E′), Vasa (magenta in D and E), and Hts and FasIII (gray in D′′ and E′′). Scale bars: 10 μm.

A

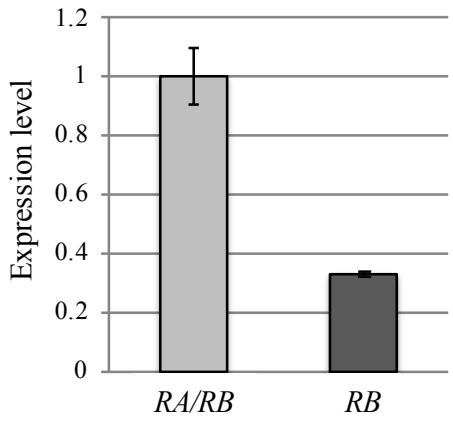
1.2
1
0.8
0.6
0.4
0.2
0
Expression level
RA/RB
RB

B

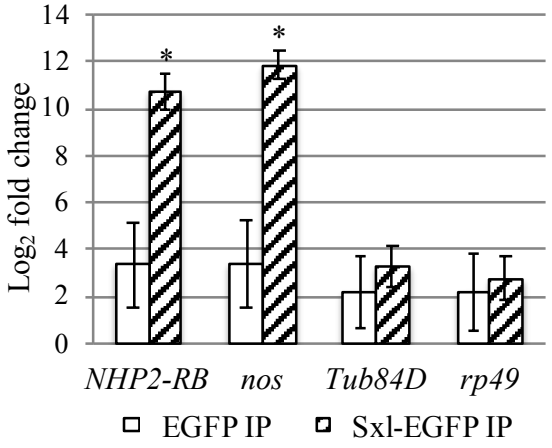
14
12
10
8
6
4
2
0
Log2 fold change
*
*
NHP2-RB
nos
Tub84D
rp49
EGFP IP
Sxl-EGFP IP

Fig. II-7. Binding of Sxl protein to *NHP2* mRNA in oogenesis.

(A) Expression level of both *NHP2-RA* and *NHP2-RB* mRNA (*RA/RB*, light gray) and *NHP2-RB* mRNA (*RB*, dark gray) in *bam* mutant ovaries. To detect mRNA levels, qRT-PCR was performed on cDNA derived from *bam* mutant ovaries. Average expression levels are presented in arbitrary units. Error bars indicate standard error of three biological replicates. (B) UV-crosslinked RNA immunoprecipitation (CLIP) was performed using extracts obtained from adult ovaries from *nos-Gal4*, *nos-Gal4 UASp-EGFP*, and *nos-Gal4 UASp-EGFP-Sxl* females (Table 1-5). RT-qPCR assay to detect *NHP2-RB*, *nos* (a positive control), *Tub84D*, and *rp49* (negative controls) mRNA were performed using 10% of total extract (10% input) and samples immunoprecipitated with anti-GFP antibody. The amount of each RNA in the immunoprecipitated samples from *nos-Gal4, nos-Gal4 UASp-EGFP* (EGFP IP), and *nos-Gal4 UASp-Sxl-EGFP* (Sxl-EGFP IP) ovaries was normalized against the corresponding amount of RNA in the 10% input, and the average enrichment ($\log_2$ fold change) of each RNA in EGFP IP (open bars) and Sxl-EGFP IP (hatched bars) in comparison with *nos-Gal4* immunoprecipitate is shown. Error bars indicate standard error of three biological replicates. Significance of the difference relative to EGFP IP was calculated by Student's t-test (* $P < 0.05$).

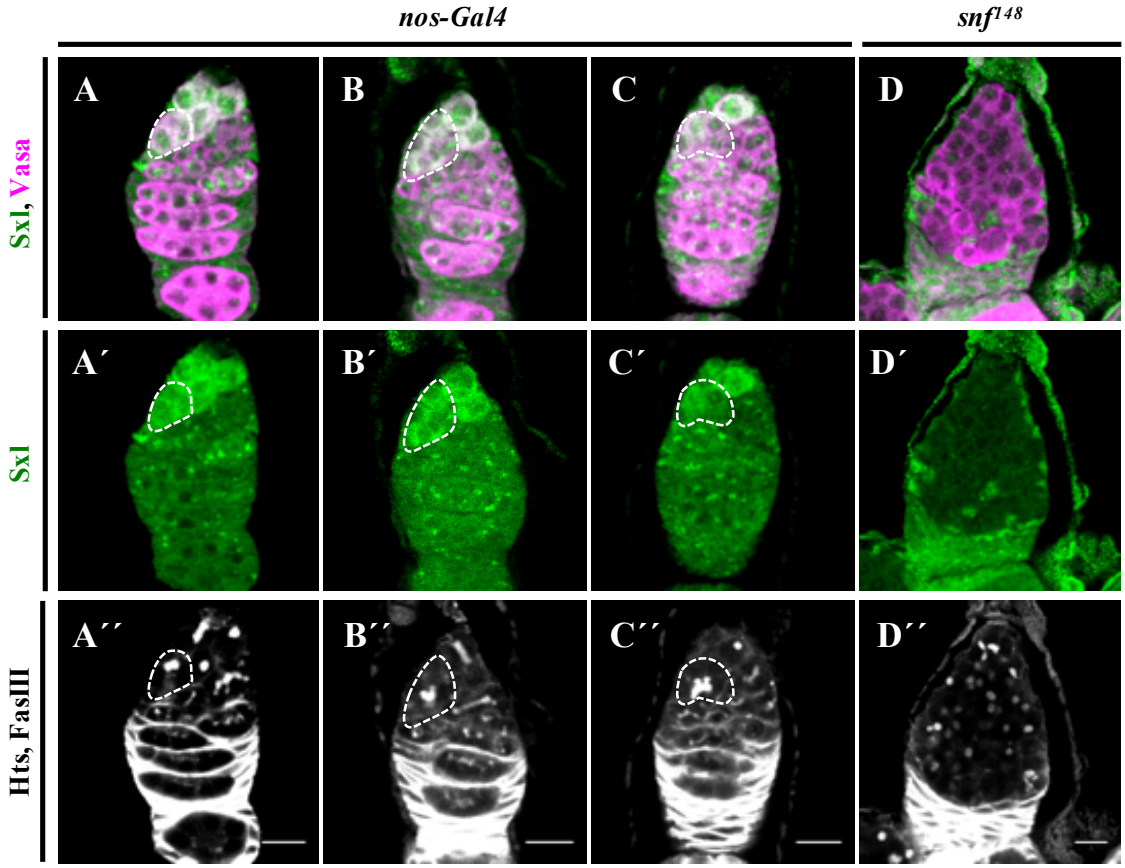
nos-Gal4
snf148
Sxl, Vasa
Sxl
Hts, FasIII
A
B
C
D
A´
B´
C´
D´
A´´
B´´
C´´
D´´

Figure II-8. Expression of Sxl protein in germarium.

(A–A′′, B–B′′, C–C′′ and D–D′′) *nos-Gal4* (A–A′′, B–B′′ and C–C′′) and *snf*^{148} germarium, (D–D′′) immunostained for Sxl (green in A–D and A′–D′), Vasa (magenta in A–D), and Hts and FasIII (gray in A′′–D′′). White dotted circles indicate 2-cell (A–A′′), 4-cell (B–B′′) and 8-cell cysts (C-C′′). For the negative control, we used *snf*^{148} to eliminate Sxl protein expression in germline cells (Nagengast et al., 2003; Chau et al., 2009). Scale bars: 10 μm.

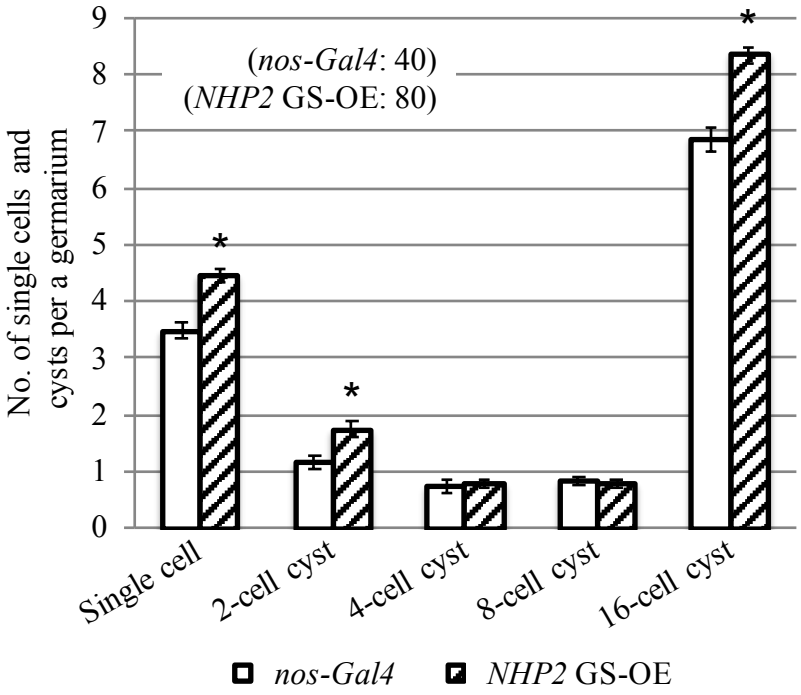
(nos-Gal4: 40)
(NHP2 GS-OE: 80)
No. of single cells and cysts per a germarium
9
8
7
6
5
4
3
2
1
0
*
*
*
Single cell
2-cell cyst
4-cell cyst
8-cell cyst
16-cell cyst
nos-Gal4
NHP2 GS-OE

Figure II-9. Defects in cyst formation in *NHP2* GS-OE germarium.
Average numbers of single cells and 2-, 4-, 8-, and 16-cell cysts per germarium from *nos-Gal4* (open bars) and *NHP2* GS-KD females (hatched bars) are indicated. Error bars indicate standard error. Significance of the difference relative to *nos-Gal4* was calculated by Student's t-test (* $P < 0.05$). The number of germaria examined is shown in parentheses. The numbers of single cells and 2-cell cysts were increased in *NHP2* GS-OE germarium, compared with *nos-Gal4.* In addition, the number of 16-cell cysts was also increased in *NHP2* GS-OE germarium, suggesting that NHP2 expression facilitates progression to 16-cell cysts.

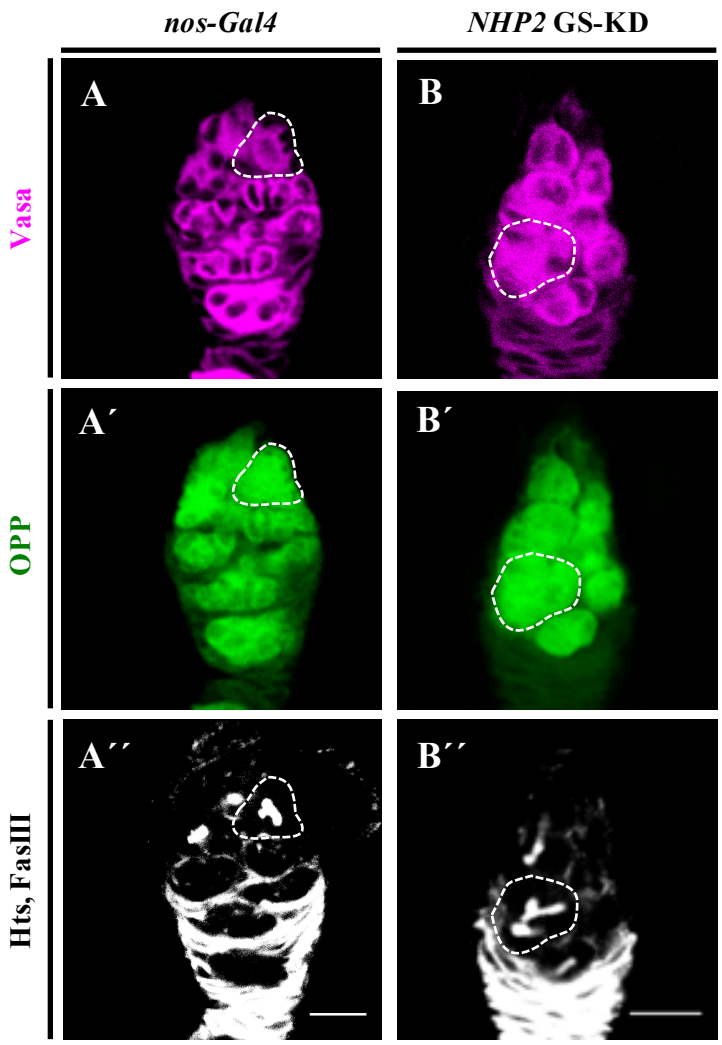
nos-Gal4
NHP2 GS-KD
A
B
Vasa
A´
B´
OPP
A´´
B´´
Hts, FasIII

Figure II-10. OPP staining in *NHP2* GS-KD germarium.

(A–A′′ and B–B′′) *nos-Gal4* (A–A′′) and *NHP2* GS-KD germarium (B–B′′) immunostained for Vasa (magenta in A and B), OPP (green in A′ and B′) and Hts and FasIII (gray in A′′ and B′′). White dotted circles indicate 8-cell cysts. Scale bars: 10 μm.

Table II-1. Primer sequences for transgene construction and FISH

Primer name	Primer sequence (5′–3′) †
NHP2-EGFP-sgRNA-Fw	CTTCGGATCTGTACGACGAGGTCA
NHP2-EGFP-sgRNA-Rv	AAACTGACCTCGTCGTACAGATCC
pEGFP-N1-Fw	**C**CTGTACGA**T**GAGGT**G**AAGGAGGAGCTGTCTGCACTAAACATACCCGTC*GCC*GCCGTGAGCAAGGGCGAGGAGC
pEGFP-N1-Rv	TAGCCGATGGAACTAATCCTACAGATTTACTTGTACAGCTCGTCCATGC
NHP2-upstream-1kb-Fw	ACGACTCACTATAGGGCGAATTGGAATATTATCCAACTGGCCAAGC
NHP2-upstream-1kb-Rv	CTCCTCCTT**C**ACCTC**A**TCGTACAG**G**TCCTTGTACTCCTCGTTCTGG
NHP2-downstream-1kb-Fw	GCATGGACGAGCTGTACAAGTAAATCTGTAGGATTAGTTCCATCGGCTA
NHP2-downstream-1kb-Rv	CCTCACTAAAGGGAACAAAAGCTGGGCTAGCGACTTGGATAGCGTAAACA
pBlue-Fw	TGTTTACGCTATCCAAGTCGCTAGCCCAGCTTTTGTTCCCTTTAGTGAGG
pBlue-Rv	GCTTGGCCAGTTGGATAATATTCCAATTCGCCCTATAGTGAGTCGT
NHP2-RA-Fw	AGGTCCTGTTCATTGCAAAATGGGCAAAGTGAAAGTAGA
NHP2-RA-Rv	GTGGCCTATGCGGCCCTAGACGGGTATGTTTAGTG
NHP2-FISH-Fw	ACACGTGTTTCGAACAAAAAGC
NHP2-FISH-Rv	GCCGATGGAACTAATCCTACAGA

† The overlapping ends for Gibson Assembly are underlined. To avoid re-cutting of the knock-in allele by gRNA and Cas9, synonymous base substitutions were introduced (bold). To express NHP2-EGFP fusion protein, the stop codon of *NHP2* and start codon of EGFP were replaced with alanine, indicated in italics and double underline, respectively. To express the transgene efficiently, kozac sequence, which is indicated by shaded text, was inserted into *UASp-NHP2*.

Table II-2. Primer sequences for RT-PCR and RT-qPCR

Primer name	Primer sequence (5′–3′)
NHP2-qPCR-Fw	CCAATAAACTTCGGAGAATGCC
NHP2-qPCR-Rv	TGTAAGCACCATCTGCCTAGACTC
NHP2-RARB-abs-qPCR-Fw	GGAGTCCTACGACGACAAG
NHP2-RARB-abs-qPCR-Rv	GTCCATTTCGCAGGAAAGTC
NHP2-RB-abs-qPCR-Fw	CCAATAAACTTCGGAGAATGCC
NHP2-RB-abs-qPCR-Rv	TAAGCACCATCTGCCTAGACTC
nos-qPCR-Fw	ACACATGAAACAACCGCCAG
nos-qPCR-Rv	TATTTGGCACTCGAGCCATTG
Tub84D-qPCR-Fw	CCGAAACCTGGACATCGAAC
Tub84D-qPCR-Rv	CCACATTTAGGGCTCCATCG
rp49-qPCR-Fw	AGTCGGATCGATATGCTAAGCTG
rp49-qPCR-Rv	ATGTTGGGCATCAGATACTGTCC

Table II-3. Number of Bam-positive cysts in *nos-Gal4* and *NHP2* GS-KD germaria

	4-cell cysts / germarium		8-cell cysts / germarium	
Ovaries[†]	Total	Bam^+ cysts	Total	Bam^+ cysts
nos-Gal4	0.88 ± 0.20	0.88 ± 0.20	0.75 ± 0.17	0.75 ± 0.17
NHP2 GS-KD	2.11 ± 0.38	0.79 ± 0.32 *	2.79 ± 0.27	1.79 ± 0.27 **

[†]*NHP2* GS-KD ovaries were obtained from the females derived from *nos-Gal4*/*nos-Gal4* females mated with $UAS\text{-}NHP2^{RNAi}$/$UAS\text{-}NHP2^{RNAi}$ males. Ovaries were dissected from adults 5–10 days after eclosion, and stained for Bam, Hts, FasIII, and Vasa. Average numbers (± standard error) of Bam-positive and -negative cysts (Total) and Bam-positive cysts (Bam^+ cysts) per germarium were calculated. A total of 16 *nos-Gal4* germaria and 19 *NHP2* GS-KD germaria were examined. Bam-positive cysts were defined as those in which Bam staining was more intense than in the germline cells adjacent to the niche. * $P > 0.05$, ** $P < 0.05$: Significance of the difference relative to the *nos-Gal4* was calculated using Student's t-test.

Table II-4. Number of Bam-positive cysts in *Sxl* GS-KD and *NHP2-Sxl* GS-KD germaria

	4-cell cysts / germarium		8-cell cysts / germarium	
Ovaries[†]	Total	Bam^+ cysts	Total	Bam^+ cysts
Sxl GS-KD	1.50 ± 0.20	0.70 ± 0.20	1.30 ± 0.17	0.10 ± 0.17
NHP2-Sxl GS-KD	4.64 ± 0.38	1.36 ± 0.32 *	4.45 ± 0.27	2.36 ± 0.27 **

[†]*Sxl* GS-KD ovaries were obtained from females derived from *nos-Gal4*/*nos-Gal4* females mated with *UAS-*Sxl^{RNAi}/*UAS-*Sxl^{RNAi} males. *NHP2-Sxl* GS-KD ovaries were obtained from females derived from *nos-Gal4*/*nos-Gal4* females mated with *UAS-*$NHP2^{RNAi}$/*UAS-*$NHP2^{RNAi}$; *UAS-*Sxl^{RNAi}/*UAS-*Sxl^{RNAi} males. Ovaries were dissected from adults 5–10 days after eclosion, and stained for Bam, Hts, FasIII, and Vasa. Average numbers (± standard error) of Bam-positive and -negative cysts (Total) and Bam-positive cysts (Bam^+ cysts) per germarium were calculated. A total of 19 *Sxl* GS-KD germaria and 11 *NHP2-Sxl* GS-KD germaria were examined. Bam-positive cysts were defined as those in which Bam staining was more intense than in the germline cells adjacent to the niche. * $P > 0.05$, ** $P < 0.05$: Significance of the difference relative to the *Sxl* GS-KD was calculated using Student's t-test

Table II-5. **Abbreviations and genotypes**

Abbreviations	Genotypes
NHP2-EGFP	+ / + ; *NHP2-EGFP* / *NHP2-EGFP*
NHP2 GS-KD	*UAS-NHP2*^{RNAi} / + ; *nos-Gal4* / +
NHP2 GS-OE	*UASp-NHP2* / +; *nos-Gal4* / +
Sxl GS-KD	+ / + ; *UAS-Sxl*^{RNAi} / *nos-Gal4*
NHP2-Sxl GS-KD	*UAS-NHP2*^{RNAi} / + ; *UAS-Sxl*^{RNAi} / *nos-Gal4*
nos-Gal4	+ / + ; *nos-Gal4* / *nos-Gal4*
nos-Gal4 UASp-EGFP	*UASp-Flag-GFP* / + ; *nos-Gal4* / +
nos-Gal4 UASp-Sxl-EGFP	*UASp-Flag-GFP-Sxl* / + ; *nos-Gal4* / +

Acknowledgements

I express my sincere appreciation to Dr. Satoru Kobayashi for his invaluable advice and encouragement throughout the course of this study. I am grateful to Drs. Hiroshi Wada, Ryusuke Niwa and Kentaro Nakano for helpful suggestion on this study.

I also thank to all of the following: Dr. Ryoma Ota for teaching me the experimental procedures; all the members of the laboratory for all kinds of support; Dr. Hirosi Sakamoto for providing anti-Sxl antibody; Dr. Akira Nakamura for providing *pgc* $^{\Delta 1}$ strain; Bloomington *Drosophila* Stock Center for providing *Drosophila* stocks and Developmental Studies Hybridoma Bank for providing antibodies. Lastly, I would like to thank my family for their support during this study.

References

Bashaw, G. J. and Baker, B. S. (1997). The Regulation of the *Drosophila msl-2* Gene Reveals a Function for *Sex-lethal* in Translational Control. *Cell* **89**, 789–798.

Beckmann, K., Grskovic, M., Gebauer, F. and Hentze, M. W. (2005). A Dual Inhibitory Mechanism Restricts *msl-2* mRNA Translation for Dosage Compensation in *Drosophila*. *Cell* **122**, 529–540.

Bopp, D., Bell, L. R., Cline, T. W. and Schedl, P. (1991). Developmental distribution of female-specific Sex-lethal proteins in *Drosophila melanogaster*. *Genes Dev.* **5**, 403–415.

Bousquet-Antonelli, C., Henry, Y., Gélugne, J. P., Caizergues-Ferrer, M. and Kiss, T. (1997). A small nucleolar RNP protein is required for pseudouridylation of eukaryotic ribosomal RNAs. *EMBO J.* **16**, 4770–4776.

Chau, J., Kulnane, L. S. and Salz, H. K. (2009). *Sex-lethal* facilitates the transition from germline stem cell to committed daughter cell in the *Drosophila* ovary. *Genetics* **182**, 121–132.

Chau, J., Kulnane, L. S. and Salz, H. K. (2012). *Sex-lethal* enables germline stem cell differentiation by down-regulating Nanos protein levels during *Drosophila* oogenesis. *Proc. Natl. Acad. Sci.* **109**, 9465–9470.

Chen, D. and McKearin, D. M. (2003a). A discrete transcriptional silencer in the bam gene determines asymmetric division of the *Drosophila* germline stem cell. *Development* **130**, 1159–1170.

Chen, D. and McKearin, D. (2003b). Dpp Signaling Silences bam Transcription Directly to Establish Asymmetric Divisions of Germline Stem Cells. *Curr. Biol.* **13**, 1786–1791.

de Cuevas, M., Lilly, M. and Spradling, A. (1997). Germline Cyst Formation in *Drosophila*. *Annu. Rev. Genet.* **31**, 405–428.

Duncan, K., Grskovic, M., Strein, C., Beckmann, K., Niggeweg, R., Abaza, I., Gebauer, F., Wilm, M. and Hentze, M. W. (2006). Sex-lethal imparts a sex-specific function to UNR by recruiting it to the *msl-2* mRNA 3' UTR: translational repression for dosage compensation. *Genes Dev.* **20**, 368–379.

Duncan, K. E., Strein, C. and Hentze, M. W. (2009). The SXL-UNR Corepressor Complex Uses a PABP-Mediated Mechanism to Inhibit Ribosome Recruitment to *msl-2* mRNA. *Mol. Cell* **36**, 571–582.

Ganot, P., Bortolin, M.-L. and Kiss, T. (1997). Site-Specific Pseudouridine Formation in Preribosomal RNA Is Guided by Small Nucleolar RNAs. *Cell* **89**, 799–809.

Ge, J. and Yu, Y. T. (2013). RNA pseudouridylation: New insights into an old modification. *Trends Biochem. Sci.* **38**, 210–218.

Gilbert, W. V. (2011). Functional specialization of ribosomes? *Trends Biochem. Sci.*

36, 127–132.

Gokcezade, J., Sienski, G. and Duchek, P. (2014). Efficient CRISPR/Cas9 Plasmids for Rapid and Versatile Genome Editing in *Drosophila*. *G3 (Bethesda).* **4**, 2279–2282.

Hayashi, Y., Hayashi, M. and Kobayashi, S. (2004). Nanos suppresses somatic cell fate in *Drosophila* germ line. *Proc. Natl. Acad. Sci. U. S. A.* **101**, 10338–42.

Henras, A., Henry, Y., Bousquet-Antonelli, C., Noaillac-Depeyre, J., Gélugne, J. P. and Caizergues-Ferrer, M. (1998). Nhp2p and Nop10p are essential for the function of H/ACA snoRNPs. *EMBO J.* **17**, 7078–90.

Jack, K., Bellodi, C., Landry, D. M., Niederer, R. O., Meskauskas, A., Musalgaonkar, S., Kopmar, N., Krasnykh, O., Dean, A. M., Thompson, S. R., et al. (2011). rRNA Pseudouridylation Defects Affect Ribosomal Ligand Binding and Translational Fidelity from Yeast to Human Cells. *Mol. Cell* **44**, 660–666.

Keyes, L. N., Cline, T. W. and Schedl, P. (1992). The Primary Sex Determination Signal of *Drosophila* Acts at the Level of Transcription. *Cell* **68**, 933–943.

Kierzek, E., Malgowska, M., Lisowiec, J., Turner, D. H., Gdaniec, Z. and Kierzek, R. (2014). The contribution of pseudouridine to stabilities and structure of RNAs. *Nucleic Acids Res.* **42**, 3492–3501.

Kirilly, D. and Xie, T. (2007). The *Drosophila* ovary: an active stem cell community. *Cell Res.* **17**, 15–25.

Li, Y., Minor, N. T., Park, J. K., McKearin, D. M. and Maines, J. Z. (2009). Bam and Bgcn antagonize *Nanos*-dependent germ-line stem cell maintenance. *Proc. Natl. Acad. Sci. U. S. A.* **106**, 9304–9.

Li, Y., Zhang, Q., Carreira-Rosario, A., Maines, J. Z., McKearin, D. M. and Buszczak, M. (2013). Mei-P26 Cooperates with Bam, Bgcn and Sxl to Promote Early Germline Development in the *Drosophila* Ovary. *PLoS One* **8**, e58301.

Lin, H. (1997). THE TAO OF STEM CELLS IN THE GERMLINE. *Annu. Rev. Genet.* **31**, 455–91.

Lin, H., Yue, L. and Spradling, A. C. (1994). The *Drosophila* fusome, a germline-specific organelle, contains membrane skeletal proteins and functions in cyst formation. *Development* **120**, 947–56.

Liu, J., Xu, Y., Stoleru, D. and Salic, A. (2012). Imaging protein synthesis in cells and tissues with an alkyne analog of puromycin. *Proc. Natl. Acad. Sci. U. S. A.* **109**, 413–418.

Lucchesi, J. C. and Kuroda, M. I. (2015). Dosage compensation in *Drosophila*. *Cold Spring Harb. Perspect. Biol.* **7**, a019398.

Maiorano, D., Brimage, L. J., Leroy, D. and Kearsey, S. E. (1999). Functional Conservation and Cell Cycle Localization of the Nhp2 Core Component of H + ACA snoRNPs in Fission and Budding Yeasts. *Exp. Cell Res.* **252**, 165–74.

McKearin, D. and Ohlstein, B. (1995). A role for the *Drosophila* Bag-of-marbles

protein in the differentiation of cystoblasts from germline stem cells. *Development* **121**, 2937–2947.

McKearin, D. M. and Spradling, A. C. (1990). bag-of-marbles: A *Drosophil*a gene required to initiate both male and female gametogenesis. *Genes Dev.* **4**, 2242–2251.

Ni, J., Tien, A. L. and Fournier, M. J. (1997). Small Nucleolar RNAs Direct Site-Specific Synthesis of Pseudouridine in Ribosomal RNA. *Cell* **89**, 565–573.

Ohlstein, B. and McKearin, D. (1997). Ectopic expression of the *Drosophila* Bam protein eliminates oogenic germline stem cells. *Development* **124**, 3651–62.

Ota, R., Morita, S., Sato, M., Shigenobu, S., Hayashi, M. and Kobayashi, S. (2017). Transcripts immunoprecipitated with Sxl protein in primordial germ cells of *Drosophila* embryos. *Dev. Growth Differ.* **59**, 713–723.

Penalva, L. O. F. and Sánchez, L. (2003). RNA Binding Protein Sex-Lethal (Sxl) and Control of *Drosophila* Sex Determination and Dosage Compensation. *Microbiol. Mol. Biol. Rev.* **67**, 343–359.

Pogacic, V., Dragon, F. and Filipowicz, W. (2000). Human H/ACA Small Nucleolar RNPs and Telomerase Share Evolutionarily Conserved Proteins NHP2 and NOP10. *Mol. Cell. Biol.* **20**, 9028–9040.

Robinson, D. N., Cant, K. and Cooley, L. (1994). Morphogenesis of *Drosophila* ovarian ring canals. *Development* **120**, 2015–2025.

Rørth, P. (1998). Gal4 in the *Drosophila* female germline. *Mech. Dev.* **78**, 113–118.

Sanchez, C. G., Teixeira, F. K., Czech, B., Preall, J. B., Zamparini, A. L., Seifert, J. R. K., Malone, C. D., Hannon, G. J. and Lehmann, R. (2016). Regulation of Ribosome Biogenesis and Protein Synthesis Controls Germline Stem Cell Differentiation. *Cell Stem Cell* **18**, 276–290.

Schindelin, J., Arganda-Carreras, I., Frise, E., Kaynig, V., Longair, M., Pietzsch, T., Preibisch, S., Rueden, C., Saalfeld, S., Schmid, B., et al. (2012). Fiji: an open-source platform for biological-image analysis. *Nat. Methods* **9**, 676–682.

Kelley, R. L., Wang, J., Bell, L. and Kuroda, M. I. (1997). *Sex lethal* controls dosage compensation in *Drosophila* by a non-splicing mechanism. *Nature* **387,** 195-199.

Song, X., Wong, M. D., Kawase, E., Xi, R., Ding, B. C., McCarthy, J. J. and Xie, T. (2004). Bmp signals from niche cells directly repress transcription of a differentiation-promoting gene, *bag of marbles*, in germline stem cells in the *Drosophila* ovary. *Development* **131**, 1353–1364.

Spradling, A., Fuller, M. T., Braun, R. E. and Yoshida, S. (2011). Germline Stem Cells. *Cold Spring Harb. Perspect. Biol.* **3**, a002642–a002642.

Steinmann-Zwicky, M., Schmid, H. and Nöthiger, R. (1989). Cell-Autonomous and Inductive Signals Can Determine the Sex of the Germ Line of *Drosophila* by Regulating the Gene *Sxl*. *Cell* **57**, 157–166.

Watkins, N. J. and Bohnsack, M. T. (2012). The box C/D and H/ACA snoRNPs: Key

players in the modification, processing and the dynamic folding of ribosomal RNA. *Wiley Interdiscip. Rev. RNA* **3**, 397–414.

Werner, A., Iwasaki, S., McGourty, C. A., Medina-Ruiz, S., Teerikorpi, N., Fedrigo, I., Ingolia, N. T. and Rape, M. (2015). Cell-fate determination by ubiquitin-dependent regulation of translation. *Nature* **525**, 523–527.

Xi, R., Doan, C., Liu, D. and Xie, T. (2005). Pelota controls self-renewal of germline stem cells by repressing a Bam-independent differentiation pathway. *Development* **132**, 5365–5374.

Xie, T. and Spradling, A. C. (1998). *decapentaplegic* is Essential for the Maintenance and Division of Germline Stem Cells in the *Drosophila* Ovary. *Cell* **94**, 251–260.

Xue, S. and Barna, M. (2012). Specialized ribosomes: a new frontier in gene regulation and organismal biology. *Nat. Rev. Mol. Cell Biol.* **13**, 355–369.

Yoon, A., Peng, G., Brandenburg, Y., Zollo, O., Xu, W., Rego, E. and Ruggero, D. (2006). Impaired Control of IRES-Mediated Translation in X-Linked Dyskeratosis Congenita. *Science.* **312**, 902–906.

Zhang, Q., Shalaby, N. A. and Buszczak, M. (2014). Changes in rRNA Transcription Influence Proliferation and Cell Fate Within a Stem Cell Lineage. *Science.* **343**, 298–301.